

# *Min*BAD: The Minimum-Biased Anisotropic Diffusion for Noise Removal\*

Seongjai Kim<sup>†</sup>, Ionut Emil Iacob<sup>‡</sup> and Matthew Tynan<sup>§</sup>

## Abstract

One of most challenging problems in image processing is edge-preserving noise removal, because edges deliver most important information to the human visual system. The article is concerned with efficient numerical techniques for edge-preserving noise removal, solving nonlinear partial differential equations. A new minimum-biased anisotropic diffusion (MinBAD) algorithm is introduced to efficiently eliminate the noise and to minimize diffusion on both the piecewise smooth portions and their boundaries. It has been numerically verified that MinBAD eliminates, rather than diffuses, the noise and shows great properties in image restoration. It is compared with various median filters. MinBAD turns out to be better than most median filters and an optimal performance is observed when the permutation center weighted median filter is adopted as a post-processor of MinBAD.

**Key words.** Noise removal, image restoration, anisotropic diffusion, median filter, minimum-biased finite difference, locally one-dimensional time-stepping procedure.

---

\*Technical Report #02-06, Department of Mathematics, University of Kentucky, Lexington, KY 40506

<sup>†</sup>Department of Mathematics, University of Kentucky, Lexington, Kentucky 40506-0027 USA  
Email: skim@ms.uky.edu. The work of this author is supported in part by NSF grant DMS-0107210.

<sup>‡</sup>Department of Mathematics, University of Kentucky, Lexington, Kentucky 40506-0027 USA  
Email: ionut@ms.uky.edu

<sup>§</sup>MSTC, Paul Laurence Dunbar High School, 1600 Man O' War Blvd, Lexington, KY 40513 USA  
Email: matthewtynan@yahoo.com

## Contents

<b>1. Introduction</b>	<b>3</b>
<b>2. Preliminaries</b>	<b>4</b>
2.1. Nonlinear median filters . . . . .	4
2.2. PDE-based approaches . . . . .	6
2.3. Desirable numerical properties . . . . .	7
<b>3. Minimum-Biased Anisotropic Diffusion</b>	<b>8</b>
3.1. An observation . . . . .	8
3.2. The one-sided difference formula . . . . .	9
3.3. The Crank-Nicolson ADI procedure . . . . .	10
3.4. Numerical experiments with <i>MinBAD</i> . . . . .	11
<b>4. The Hybrid Algorithm</b>	<b>13</b>
<b>5. Numerical Experiments</b>	<b>15</b>
<b>6. Conclusions</b>	<b>17</b>

## 1. Introduction

In the modern digital age, many applications are based on images and therefore the resulting achievements must rely on their quality. Since images are not always in a good quality due to various types of noise (natural noise, defects in the sensors, transmission problems, etc.), it is important to remove the noise automatically and efficiently. Image restoration is historically one of the oldest concerns and still a necessary processing step for many other applications, as indicated in [3]. As the field requires higher levels of *reliability* and *efficiency* for the last two decades, mathematical image processing has become an important component. In particular, mathematical frameworks employing recent powerful theory of partial differential equations (PDEs) and functional analysis have been extensively studied to answer fundamental questions in image processing.

Applications of the PDE models can be widely found in a broad range of image processing tasks such as denoising, deblurring, object and pattern recognition, segmentation, matching, and morphing. These can be categorized to three major parts: image restoration, segmentation, and compression. Image restoration is often necessary as a pre-processing for segmentation and compression; good denoising methods have strong demands. However, those PDE-based methods can show some drawbacks unless the governing equations are incorporating appropriate parameters and discretized by suitable numerical schemes. The selected model parameters and numerical schemes should be able to capture characteristics of the image. The development of appropriate numerical techniques for the PDE models is another important component of PDE-based approaches.

There are other ways to tackle image restoration; among others, we quote the filtering approaches [2, 5, 15, 20, 30] and stochastic modeling [4, 8, 14] for interested readers.

Edges deliver most important information of images to the human visual system (HVS). Thus one of the biggest issues in image analysis is how to preserve or enhance edges. The article is concerned with efficient PDE-based numerical techniques for edge-preserving denoising. For an effective noise removal with the anisotropic mean-curvature flow, we introduce a new minimum-biased FD scheme to minimize diffusion on both the piecewise smooth portions and their boundaries. For the time-stepping procedure, the incomplete alternating direction implicit (ADI) method is considered along with formulas for effective time-step sizes, both to remove the high-frequency components of the error (the noise) more efficiently and to minimize the torture of lower-frequency components of the image. Also we discuss a strategy for automatic stop of the diffusion process. The overall algorithm, called the minimum-biased anisotropic diffusion (MinBAD), has been numerically verified that it elimi-

nates, rather than diffuses, the noise and turns out to be better than most median filters. When median filters are applied as a post-processing, the algorithm improves its performance.

An outline of the article is as follows. In the next section, we review briefly median filters [2, 5, 15, 17, 30, 34] and PDE-based approaches [1, 6, 7, 24, 27, 35]. The section also includes a set of desirable properties for image restoration algorithms. Section 3 presents a refinement of the so-called *Minimum-Biased Anisotropic Diffusion* (*MinBAD*) [16], which satisfies the set of desirable properties for various realistic images. The new algorithm incorporates minimum-biased difference formula, Crank-Nicolson-ADI time-stepping procedure, and a strategy of choosing optimal timestep size. In Section 4, we present a hybrid algorithm where the permutation center-weighted median (PCWM) filter is adopted as a post-process for *MinBAD*. Section 5 presents numerical experiments with the hybrid algorithm, which shows a better performance than a sole application of *MinBAD* and the PCWM filter, for the removal of impulse noise and Gaussian noise. The last section concludes our experiments.

## 2. Preliminaries

In this section, we review some of conventional approaches for image denoising/enhancement, focusing on median filters and PDE-based approaches. We also consider desirable properties for noise removal algorithms.

### 2.1. Nonlinear median filters

The median filter (called the *running median*) was first suggested as a nonlinear smoother for discrete data by Tukey in 1974 [30]. Since then, variants have been studied to attenuate high-frequency noise more effectively and preserve signal edges better. Weighted median filters were introduced in the signal processing literature by Brownrigg in 1984 [5] and have been received a considerable attention [17, 34]. The performance of those nonlinear smoothers has been further improved by incorporating ways of rank-dependent weight section, as in *permutation weighted median filters* [2, 15]. See also Mitra and Sicuranza [20].

The nonlinear median filters show good properties in suppressing impulse noise, while preserving the signal edges well, especially when the impulses occur with relatively low probabilities.

In Figure 1, we present performance of median filters suppressing impulse noise. The Lena image is perturbed by random-valued impulse noise of probability 20% and restored by the running median, center weighted median (CWM), and permutation center weighted median (PCWM) filters, for  $5 \times 5$  window. For CWM, we set the



Figure 1: The Lena images in  $256 \times 256$  cells, with (a) random-valued impulse noise of probability 20%, and restored images by the running (b) median, (c) CWM, and (d) PCWM filters. The window size is  $5 \times 5$  for the median filters.

center weight  $W_c = 15$ ; the PCWM incorporates

$$W_c = \begin{cases} 15, & \text{if } 6 \leq R_c(\mathbf{x}_{ij}) \leq 20, \\ 1, & \text{otherwise,} \end{cases} \quad (2.1)$$

where  $R_c(\mathbf{x}_{ij})$  denotes the rank of the center sample of the window at location  $\mathbf{x}_{ij}$ . As one can see from the figure, the running median smoother suppresses the noise well, but the image becomes too much blurry. The CWM filter preserves the edges relatively well; the output still contains much impulse noise. The output of the PCWM filter is less blurry than that of the running median filter and less noisy than the CWM output. However, when the noise level is relatively high, these median filters tend to remove details from the image or leave much impulse noise and the edges easily become either jagged or blurry. Their main drawback is “blindness in the spatial ordering” of signal samples. See [20] for details.

## 2.2. PDE-based approaches

Anisotropic diffusion has been a popular tool for noise removal since the first elegant formulation by Perona and Malik in 1990 [24]. A considerable amount of research has been carried out for the theoretical and computational understanding of the method and related methods for image enhancement [1, 6, 7, 19, 21, 27, 35]; good references to work on them are Osher and Fedkiw [22], Sapiro [28], and Sethian [29].

It is now well known that by choosing a proper energy functional in the variational formulation, edges in noisy images can be well restored and enhanced. Among the many possible choices, the *total variation* (TV) is one of the simplest but sufficiently efficient measurement for denoising/enhancement.

Let  $\Omega$  be a rectangular domain in  $\mathbb{R}^2$ . Suggested by Rudin, Osher and Fatemi [25, 26], for given noisy image  $u_0 : \Omega \rightarrow \mathbb{R}$ , the TV minimization is to find  $u$  which satisfies

$$\min_u F(u), \quad F(u) := \int_{\Omega} |\nabla u| d\mathbf{x} + \frac{\lambda}{2} \int_{\Omega} |u - u_0|^2 d\mathbf{x}, \quad (2.2)$$

where  $\lambda \geq 0$  is a parameter to be appropriately chosen. The Euler-Lagrange equation of the functional, parameterizing the descent direction by an artificial time  $t$ , reads

$$u_t = \nabla \cdot \left( \frac{\nabla u}{|\nabla u|} \right) + \lambda(u_0 - u). \quad (2.3)$$

Recently, Marquina and Osher [19] introduced a variant, by merely multiplying the right-side of the equation (2.2) by  $|\nabla u|$ :

$$u_t = |\nabla u| \nabla \cdot \left( \frac{\nabla u}{|\nabla u|} \right) + \lambda |\nabla u| (u_0 - u). \quad (2.4)$$

The authors claimed that (2.4) had the same steady state solution as (2.3) and it showed strong analytical, numerical, and philosophical advantages, because  $|\nabla u|$  vanished only in flat regions. See also [22, §11.3].

Earlier to the model (2.3) above, Perona and Malik [24] introduced an anisotropic diffusion model which aims at the enhancement of edges

$$\frac{\partial u}{\partial t} - \nabla \cdot (g(|\nabla u|) \nabla u) = 0, \quad (\mathbf{x}, t) \in \Omega \times J, \quad (2.5)$$

where  $g$  is a function,  $g(x) \geq 0$ , having the property:

$$g(x) \rightarrow 0 \quad \text{as } x \rightarrow \infty. \quad (2.6)$$

For example, one may choose one of the following

$$\begin{aligned} g(x) &= 1/(1 + x^2/\sigma^2), \\ g(x) &= e^{-x^2/\sigma^2}, \end{aligned} \quad \sigma > 0. \quad (2.7)$$

The equation (2.5) has motivated a large number of researchers to study the mathematical properties of the kind, numerical schemes, and applications [1, 6, 24].

From various experiments, we have found the following: The parameters  $\lambda$  and  $\sigma$  in (2.3), (2.4), and (2.5)-(2.7) must be chosen appropriately. For example,  $\lambda$  should be large enough to preserve high-frequency components of the image, while it must be small enough to smoothen the image. For the functions  $g$  in (2.7), the parameter  $\sigma$  must be determined based on statistical properties of the images; its choice is often problematic [16]. It should be sufficiently small to virtually stop diffusion across the edges, because otherwise edges of small jumps would smear out rapidly. On the other hand, it should be large enough to efficiently eliminate noise of high-frequency. For a fixed  $\sigma$ , the diffusion can be small at points where the gradient magnitude is large, e.g., the edges and the noise. However, the diffusion would be large where the gradient magnitude is small such as for *faces*. By *faces* we mean the piecewise smooth portions of the image. As a consequence, the diffusion process makes relatively flat portions of the image flatter, which is called the *staircase effect* in the literature [19]. Since the noise is hardly smooth, the gradient magnitude is likely large at points perturbed, in particular, by impulse noise. Thus there is possibility that the noise removal process incorporating (2.5) and (2.7) either fails or becomes extremely slow. The main goal of this article is to introduce edge-preserving algorithms which can eliminate the noise in a few iterations.

### 2.3. Desirable numerical properties

Now, we consider *desirable numerical properties* in image restoration:

$$(\mathcal{P}) \begin{cases} \text{(a) Fast removal of the } noise, \\ \text{(b) Small diffusion on the } faces, \\ \text{(c) Small diffusion on the } edges, \end{cases} \quad (2.8)$$

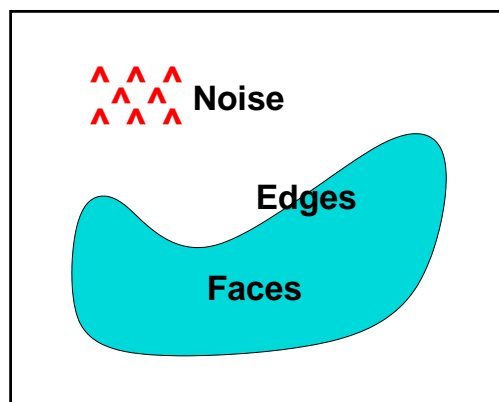


Figure 2: A symbolized image.

where *faces* denote the piecewise smooth portions of the image. See Figure 2 for a symbolized image.

Note that the nonlinear diffusion (2.5)-(2.7), applied for denoising, is hard to satisfy the properties in  $(\mathcal{P})$  except for the last one.

### 3. Minimum-Biased Anisotropic Diffusion

In this section, we review and *refine* the so-called *Minimum-Biased Anisotropic Diffusion* (*MinBAD*) [16], which satisfies each of properties in  $(\mathcal{P})$  for various realistic images. In particular, the properties will be satisfied *perfectly* for piecewise constant images. For simplicity, we derive the numerical techniques for the *motion by mean-curvature*:

$$u_t = |\nabla u| \nabla \cdot \left( \frac{\nabla u}{\|\nabla u\|} \right), \quad (3.1)$$

where  $|\nabla u|$  and  $\|\nabla u\|$  are the same gradient magnitude of  $u$ ; we denote them separately to apply different numerical schemes.

#### 3.1. An observation

The main purpose of the section is to introduce a PDE-based edge-preserving denoising algorithm. We begin with the following observation:

- (O1). The central difference scheme may not be appropriate for  $|\nabla u|$  in (3.1).
- (O2). The faces in the image (and the texture) are a combination of vertical, horizontal, and  $45^\circ$  line segments.

It is clear that numerical algorithms for (3.1) incorporating the central scheme for  $|\nabla u|$  will introduce a severe numerical dissipation everywhere, of course, including the edges. Properly chosen one-sided (ENO-type) schemes can preserve the edges more effectively.

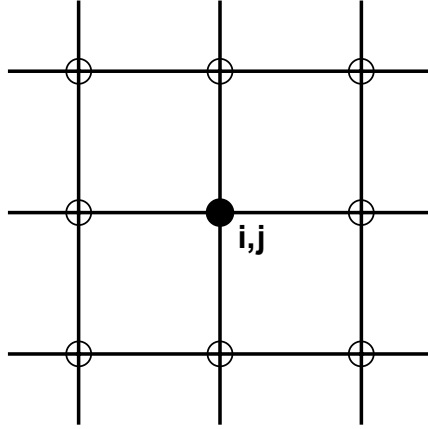


Figure 3: The grid point  $(i, j)$  and its eight neighboring points.

### 3.2. The one-sided difference formula

As a consequence of the above observation, we introduce the edge-stopping FD scheme as follows. At each grid point  $(i, j)$ , compute the *eight* one-sided differences corresponding to the eight neighboring points:

$$\frac{|u_{i,j} - u_{\ell,m}|}{\sqrt{(i-\ell)^2 + (j-m)^2}}, \quad (\ell, m) \in [i-1, i+1] \times [j-1, j+1], \quad (\ell, m) \neq (i, j). \quad (3.2)$$

(See Figure 3.) Let  $D_{ij,1}$  and  $D_{ij,2}$  ( $D_{ij,1} \leq D_{ij,2}$ ) be the two smallest quantities among the above eight differences. Then, an edge-preserving scheme for the gradient magnitude can be defined as

$$(|\nabla u|)_{i,j} \cong \sqrt{D_{ij,1}^2 + D_{ij,2}^2}, \quad (3.3)$$

which we call the *minimum-biased* (MinB) scheme.

MinB preserves piecewise constant images *perfectly*. To see this, consider a piecewise constant image. Then at least two of the one-sided FDs would be zero at each grid point and therefore the gradient magnitude in MinB becomes completely zero. On the other hand, when an isolated grid value of  $u$  differs from neighboring points, MinB is nonzero at the point and therefore the isolated value must be averaged, without introducing diffusion at adjacent points.

Note that for general images (having no noise), the tangential derivatives at the edges are small, while the normal derivative can be large. It is easy to see that at the edge points, MinB tries to evaluate the gradient magnitude  $|\nabla u|$  as an approximation of the tangential derivatives. Thus MinB would be able to preserve the edges quite well.

### 3.3. The Crank-Nicolson ADI procedure

For an efficient simulation, we may adopt the locally one-dimensional (LOD) methods such as the alternating direction implicit (ADI) method and its variants: the fractional step (FS) method [13, 18, 32, 33] and the additive operator splitting (AOS) method [31]. The ADI method was first introduced by Douglas, Peaceman, and Rachford [9, 12, 23], as a perturbation of the Crank-Nicolson difference equation, for solving the heat equation in 2D. Such LOD methods are efficient but introduce an extra error called the *splitting error*. Recently, Douglas and Kim [11] suggested a unified approach for the ADI and FS methods in which both methods are second-order accurate and their splitting errors are in third-order in time. It has been numerically verified [16] that accuracy of the numerical algorithm can affect the efficiency of noise removal and the quality of restored images. The Crank-Nicolson ADI (CN-ADI) procedure shows superior properties to other LOD methods, in both efficiency and accuracy. Also, CN-ADI allows us to choose the optimal timestep size with which the algorithm can reduce high-frequency components relatively faster than lower-frequency components.

Let  $(D_{x_1}, D_{x_2})^T$  be a proper difference operator for the gradient  $\nabla$ . Let  $\Delta t$  be the timestep size. Define  $t^n = n\Delta t$  and  $u^n = u(t^n)$ ,  $n = 0, 1, \dots$ . Consider the following *incomplete* Crank-Nicolson method for (3.1):

$$\frac{u^n - u^{n-1}}{\Delta t} + \frac{1}{2}A^{n-1}(u^n + u^{n-1}) = 0, \quad (3.4)$$

where  $A^{n-1} = A_1^{n-1} + A_2^{n-1}$ , with

$$A_\kappa^{n-1} u^n := -|\nabla_h u^{n-1}| D_{x_\kappa} \left( \frac{D_{x_\kappa} u^n}{\|\nabla_h u^{n-1}\|} \right), \quad \kappa = 1, 2.$$

Here  $|\nabla_h u^{n-1}|$  is the MinB difference of  $|\nabla u^{n-1}|$ , defined in (3.3), and the term  $\|\nabla_h u^{n-1}\|$  denotes the central difference of  $\|\nabla u^{n-1}\|$ .

Then, the CN-ADI procedure for (3.4) in its general formulation [10] reads

$$\begin{aligned} \left(1 + \frac{\Delta t}{2}A_1^{n-1}\right)v^* &= \left(1 - \frac{\Delta t}{2}A_1^{n-1} - \Delta t A_2^{n-1}\right)v^{n-1}, \\ \left(1 + \frac{\Delta t}{2}A_2^{n-1}\right)v^n &= v^* + \frac{\Delta t}{2}A_2^{n-1}v^{n-1}. \end{aligned} \quad (3.5)$$

The algorithm (3.5) which solves (3.1) and incorporates the MinB scheme for  $|\nabla u^{n-1}|$  is called the *minimum-biased anisotropic diffusion* (MinBAD). The algorithm can be

implemented as follows:

- (1) Get  $A_\kappa^{n-1}$ :  

$$\mathbf{A}[\kappa] \leftarrow A_\kappa^{n-1}, \quad \kappa = 1, 2;$$
- (2) Compute and save  $A_\kappa^{n-1}v^{n-1}$ :  

$$\mathbf{WS}[\kappa] \leftarrow \mathbf{A}[\kappa]\mathbf{V}, \quad \kappa = 1, 2;$$
- (3) Get  $(1 + \frac{\Delta t}{2}A_\kappa^{n-1})$ :  

$$\mathbf{A}[\kappa] \leftarrow (1 + \frac{\Delta t}{2}\mathbf{A}[\kappa]), \quad \kappa = 1, 2;$$
- (4) Do the  $x_1$ -sweep: (3.6)  

$$\mathbf{WS}[1] \leftarrow (\mathbf{V} - \Delta t(\frac{1}{2}\mathbf{WS}[1] + \mathbf{WS}[2]));$$

$$\mathbf{WS}[1] \leftarrow (\mathbf{A}[1])^{-1}\mathbf{WS}[1];$$
- (5) Do the  $x_2$ -sweep:  

$$\mathbf{WS}[2] \leftarrow (\mathbf{WS}[1] + \frac{\Delta t}{2}\mathbf{WS}[2]);$$

$$\mathbf{WS}[2] \leftarrow (\mathbf{A}[2])^{-1}\mathbf{WS}[2];$$
- (6) Swap the array for  $v^n$ :  

$$\mathbf{V} \leftarrow \mathbf{WS}[2];$$

(Its extension for 3D problems is straightforward.) In the above,  $\mathbf{V}$  is the array for the solution and  $\mathbf{WS}[\kappa]$  are arrays for temporary saving and the intermediate solution. Before swapping  $\mathbf{WS}[2]$  for  $v^n$  into the array  $\mathbf{V}$ , one can measure the difference between  $\mathbf{WS}[2]$  and  $v^{n-1}$  (saved in  $\mathbf{V}$ ). The measured difference can be utilized as a stopping criterion for the diffusion iteration.

Note that the system of tridiagonal matrices can be solved for five flops per point. Thus the required operations for the CN-ADI procedure become 25 flops per point in each time level. One can find from the above pseudo-code that the dimension of the required computer memory is 9 times the number of grid points. The CN-ADI procedure is quite efficient in both the operation count and the memory requirement. Strategies for choosing an optimal time-step size  $\Delta t$  and automatic stop of the diffusion can be found in [16].

### 3.4. Numerical experiments with *MinBAD*

To understand characteristics of *MinBAD*, the algorithm is implemented as in (3.6) and has been tested for various images.

Figure 4 shows a synthetic house image, of which the original image is piecewise constant. The left figure is perturbed by random-valued impulse noise of 10% probability and the right one is restored by two iterations of *MinBAD*. The relative difference between the original and the restored images turns out to be about  $3 \cdot 10^{-5}$ . We have found from this example that *MinBAD* converges fast and preserves edges quite well, at least for piecewise constant images.

Figure 5 contains small images (in  $100 \times 100$  cells); it is designed to see details of *MinBAD*'s performance. In a single iteration, *MinBAD* can eliminate most of the

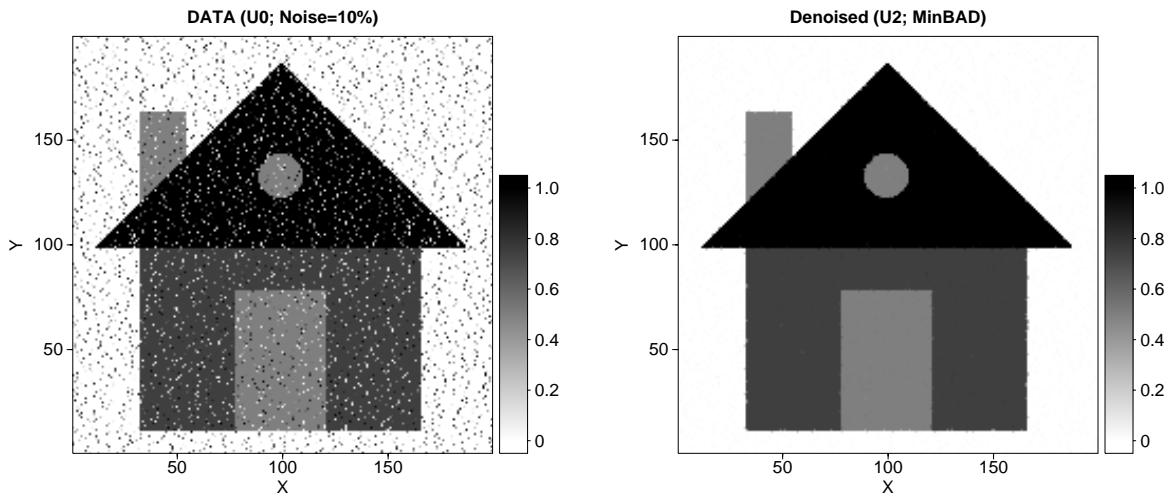


Figure 4: House images in  $200 \times 200$  cells: (left) perturbed by random-valued impulse noise of 10% probability and (right) restored by two iterations of *MinBAD*.

noise efficiently, preserving edges quite well. Thin features are destroyed in part. (*MinBAD* does not touch piecewise constant images when no noise is added.) From this example, one can see how *MinBAD* works for noise removal and the preservation of edges, along with its effectiveness and efficiency.

In Figure 6, we present Lena images that are restored by two iterations of *MinBAD* from the ones contaminated by random-valued impulse noise of 10% (left) and 20% (right) probabilities. (See Figure 1(a) for the noisy image of 20% probability.) When the random-valued noise has 10% probability, the restored image is as good as the original; in two iterations, no apparent noise is remained and the edges are well preserved. For the noise of 20% probability, *MinBAD* preserves the edges relatively well, but the noise is still remained. However, the quality of noise removal by *MinBAD* seems better than the median filters; compare the right side of Figure 6 with Figure 1(b)–(d).

To compare performances between the median filters and *MinBAD* more systematically, we have measured the differences from the original Lena image to the restored ones, as presented in Table 1. There MAE and MSE denote respectively the mean absolute ( $L^1$ ) error and the mean square ( $L^2$ ) error. As one can see from the table, *MinBAD* shows smaller residuals than median filters for all cases.

In Figure 7, we try to check *MinBAD*'s ability to handle heavier impulse noises. The Elaine image is perturbed by random-valued impulse noise of 50% probability and restored by three iterations of *MinBAD*. Although the algorithm leaves the noise in an observable amount, it seems preserving the edges well. The result is better than

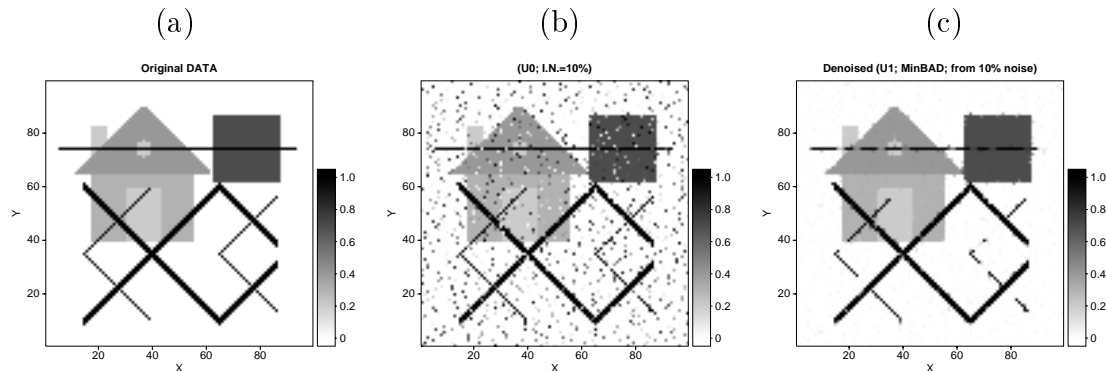


Figure 5: Images in  $100 \times 100$  cells: (a) the original image, (b) a noisy image having random-valued impulse noise of 10% probability, and (c) the image restored by one iteration of *MinBAD*.

Table 1: The error comparison between median filters and *MinBAD*.

Filters	Lena (I.N.=10%)		Lena (I.N.=20%)	
	MAE	MSE	MAE	MSE
Tukey	0.020	0.041	0.022	0.044
CWM	0.009	0.033	0.015	0.051
PCWM	0.018	0.038	0.021	0.045
MinBAD	0.009	0.025	0.012	0.029

those obtained from median filters.

We summarize the experiments presented in this section as follows:

- For piecewise constant images, *MinBAD* has shown superior properties for noise removal and edge preservation, in both effectiveness and efficiency.
- For general images, it preserves edges quite well, better than median filters.
- But, *MinBAD* still leaves some noise for highly noisy images.

#### 4. The Hybrid Algorithm

Recall that *MinBAD* preserves edges well, leaving small noise, and the PCWM filter is good for removing small impulse noise. Hence it seems natural to combine

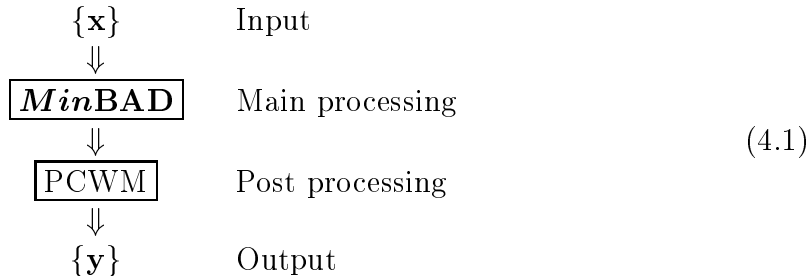


Figure 6: Lena images, restored by two iterations of *MinBAD* from the ones contaminated by random-valued impulse noise of 10% (left) and 20% (right) probabilities.



Figure 7: Elaine images in  $285 \times 283$  cells: (left) perturbed by random-valued impulse noise of 50% probability and (right) restored by three iterations of *MinBAD*.

MinBAD and PCWM as follows:



The above hybrid algorithm incorporates PCWM as a post-processor for *MinBAD*. There is no physical/practical advantage to apply them in the other way, i.e., PCWM first and followed by *MinBAD*.

## 5. Numerical Experiments

For the hybrid algorithm (4.1), all the computations are carried out on a 400MHz Laptop having a Linux operating system. The computation times to be presented in this section are measured in second for the user time.

Figure 8 shows Elaine images: (a) the noisy image perturbed by a random-valued Gaussian noise of  $\sigma^2 = 122$ , followed by a random-valued impulse noise of 33% probability; and restored images by (b) *MinBAD*, (c) PCWM, and (d) the hybrid algorithm. The right half of the restored images is replaced by the residual, the absolute distance between the original image and the restored one. PCWM incorporates  $5 \times 5$  window with the weight given in (2.1). As one can see from the figure, neither *MinBAD* nor PCWM can eliminate the noise clearly. *MinBAD* leaves the noise (spots), while PCWM has turned the noisy image jagged, during the noise removal. On the other hand, the hybrid algorithm (*MinBAD*+PCWM) has effectively restored the image, with an ignorable residual. The residual of the hybrid algorithm turns out to be smaller than those of *MinBAD* and PCWM.

We have tested the hybrid algorithm (4.1) for various images having different levels of noise. The hybrid algorithm results in superior recovery properties for most cases. For relatively smaller noise levels, the post-processor (PCWM) can be carried out with a smaller window size, e.g.,  $3 \times 3$  with the center weight

$$W_c = \begin{cases} 5, & \text{if } 3 \leq R_c(\mathbf{x}_{ij}) \leq 7, \\ 1, & \text{otherwise,} \end{cases}$$

In the case, the cost of PCWM is comparable with that of one iteration of *MinBAD*. Thus one can enjoy a similar efficiency for the hybrid algorithm as *MinBAD* itself.

In Figure 9, we present the result of the hybrid algorithm (two *MinBAD* iterations followed by PCWM having the  $3 \times 3$  window) applied for the Boat image. For



Figure 8: Elaine images: (a) the noisy image perturbed by a random-valued Gaussian noise of  $\sigma^2 = 122$ , followed by a random-valued impulse noise of 33% probability; and restored images by (b) *MinBAD*, (c) PCWM, and (d) the hybrid algorithm. In (b), (c), and (d), the right half is adjusted to show the residual.



Figure 9: The Boat images in  $256 \times 256$  cells, with (left) a random-valued impulse noise of 20% possibility and (right) restored by the hybrid algorithm. For the right figure, the right half is adjusted to show the absolute distance between the original image and the restored one.

a random-valued impulse noise of 20% possibility, the algorithm can eliminate the noise efficiently. But it also has destroyed parts of thin textures, as one can see it from the residual shown in the right half of the right figure. However, the quality of the restored image is still good and better than the result obtained from the sole application of *MinBAD* or PCWM.

## 6. Conclusions

We have numerically investigated median filters, a newly-designed PDE-based approach (*MinBAD*), and their hybrid algorithm for an efficient noise removal. We have found that the median filters are good for the removal of small amount of impulse noises, but they tend to either remove details from the image or leave much of noise. (*They are blind on the spatial ordering.*) *MinBAD* has been introduced (a) to remove the noise efficiently, (b) to minimize diffusion on piecewise smooth portions of images, and (c) to preserve edges by incorporating the tangential derivatives for the solution of the motion by mean-curvature. It turns out to eliminate the noise efficiently (in 2–3 iterations) and preserve edges quite well (perfectly, for piecewise constant images). But it has proved to leave noise when the noise level is high. (*MinBAD is rank-blind.*) To overcome the drawback observed in *MinBAD*, we have adopted the permutation center-weighted median (PCWM) filter as a post-processor of *MinBAD*. This hybrid algorithm has shown desirable properties in both noise removal and edge preservation, superior to the sole application of *MinBAD* or PCWM.

## Acknowledgment

The first author (Kim) wants to express sincere thanks to Prof. Stanley Osher, UCLA, and Prof. George Papanicolaou, Stanford University, for their constructive comments and encouragement.

## References

- [1] L. ALVAREZ, P. LIONS, AND M. MOREL, *Image selective smoothing and edge detection by nonlinear diffusion. II*, SIAM J. Numer. Anal., 29 (1992), pp. 845–866.
- [2] G. ARCE, T. HALL, AND K. BARNER, *Permutation weighted order statistic filters*, IEEE Trans. Image Process., 4 (1995), pp. 1070–1083.
- [3] G. AUBERT AND P. KORNPORST, *Mathematical Problems in Image Processing*, no. 147 in Applied Mathematics Sciences, Springer-Verlag, New York, 2002.
- [4] C. BOUMAN AND K. SAUER, *A generalized Gaussian model for edge-preserving MAP estimation*, IEEE Trans. Image Process., 2 (1993), pp. 296–310.
- [5] D. BROWNWIGG, *The weighted median filter*, Commun. Assoc. Comput. Machin., 27 (1984), pp. 807–818.
- [6] F. CATTE, P. LIONS, M. MOREL, AND T. COLL, *Image selective smoothing and edge detection by nonlinear diffusion.*, SIAM J. Numer. Anal., 29 (1992), pp. 182–193.
- [7] T. CHAN, S. OSHER, AND J. SHEN, *The digital TV filter and nonlinear denoising*, Technical Report #99-34, Department of Mathematics, University of California, Los Angeles, CA 90095-1555, October 1999.
- [8] G. DEMOMENT, *Image reconstruction and restoration: Overview of common estimation structures and problems*, IEEE Trans. Acoustics, Speech, and Signal Process., 37 (1989), pp. 2024–2036.
- [9] J. DOUGLAS, JR., *On the numerical integration of  $\frac{\partial^2 u}{\partial x^2} + \frac{\partial^2 u}{\partial y^2} = \frac{\partial u}{\partial t}$  by implicit methods*, J. Soc. Indust. Appl. Math., 3 (1955), pp. 42–65.
- [10] J. DOUGLAS, JR. AND J. GUNN, *A general formulation of alternating direction methods Part I. Parabolic and hyperbolic problems*, Numer. Math., 6 (1964), pp. 428–453.

- [11] J. DOUGLAS, JR. AND S. KIM, *Improved accuracy for locally one-dimensional methods for parabolic equations*, Mathematical Models and Methods in Applied Sciences, 11 (2001), pp. 1563–1579.
- [12] J. DOUGLAS, JR. AND D. PEACEMAN, *Numerical solution of two-dimensional heat flow problems*, American Institute of Chemical Engineering Journal, 1 (1955), pp. 505–512.
- [13] E. D'YAKONOV, *Difference schemes with split operators for multidimensional unsteady problems (English translation)*, USSR Comp. Math., 3 (1963), pp. 581–607.
- [14] S. GEMAN AND D. GEMAN, *Stochastic relaxation, Gibbs distributions, and Bayesian restoration of images*, IEEE Trans. Pattern Analysis and Machine Intelligence, 6 (1984), pp. 721–741.
- [15] R. HARDIE AND K. BARNER, *Rank conditioned rank selection filters for signal restoration*, IEEE Trans. Image Process., 3 (1994), pp. 192–206.
- [16] S. KIM, *Edge-preserving noise removal, Part I: Second-order anisotropic diffusion*. (Submitted to SIAM J. Sci. Comput.).
- [17] S.-J. KO AND Y. LEE, *Center weighted median filters and their applications to image enhancement*, IEEE Trans. Circ. Syst., 38 (1991), pp. 984–993.
- [18] G. MARCHUK, *Methods of numerical mathematics*, Springer-Verlag, New York, Heidelberg, and Berlin, 1982.
- [19] A. MARQUINA AND S. OSHER, *Explicit algorithms for a new time dependent model based on level set motion for nonlinear deblurring and noise removal*, SIAM J. Sci. Comput., 22 (2000), pp. 387–405.
- [20] S. MITRA AND G. SICURANZA, *Nonlinear Image Processing*, Academic Press, San Diego, San Francisco, New York, Boston, London, Sydney, ToKyo, 2001.
- [21] M. NITZBERG AND T. SHIOTA, *Nonlinear image filtering with edge and corner enhancement*, IEEE Trans. on Pattern Anal. Mach. Intell., 14 (1992), pp. 826–833.
- [22] S. OSHER AND R. FEDKIW, *Level Set Methods and Dynamic Implicit Surfaces*, Springer-Verlag, New York, 2003.
- [23] D. PEACEMAN AND H. RACHFORD, *The numerical solution of parabolic and elliptic equations*, J. Soc. Indust. Appl. Math., 3 (1955), pp. 28–41.

- [24] P. PERONA AND J. MALIK, *Scale-space and edge detection using anisotropic diffusion*, IEEE Trans. on Pattern Anal. Mach. Intell., 12 (1990), pp. 629–639.
- [25] L. RUDIN AND S. OSHER, *Total variation based image restoration with free local constraints*, Proc. 1st IEEE ICIP, 1 (1994), pp. 31–35.
- [26] L. RUDIN, S. OSHER, AND E. FATEMI, *Nonlinear Total Variation based Noise Removal Algorithm*, Physica D, 60 (1992), pp. 259–268.
- [27] —, *Nonlinear total variation based noise removal algorithms*, Physica D, 60 (1992), pp. 259–268.
- [28] G. SAPIRO, *Geometric partial differential equations and image analysis*, Cambridge University Press, Cambridge, 2001.
- [29] J. SETHIAN, *Level Set Methods and Fast Marching Methods (2nd Ed.)*, Cambridge University Press, Cambridge, 1999.
- [30] J. TUKEY, *Nonlinear (nonsuperposable) methods for smoothing data*, in Congr. Rec. EASCON, 1974, p. 673. (Abstract only).
- [31] J. WEICKERT, B. TER HAAR ROMENY, AND M. VIERGEVER, *Efficient and reliable schemes for nonlinear diffusion filtering*, IEEE Trans. on Image Processing, 7 (1998), pp. 398–410.
- [32] N. YANENKO, *Convergence of the method of splitting for the heat conduction equations with variable coefficients (English translation)*, USSR Comp. Math., 3 (1963), pp. 1094–1100.
- [33] —, *The method of fractional steps*, Springer-Verlag, Berlin, Heidelberg, and New York, 1971. (English translation; originally published in Russian, 1967).
- [34] L. YIN, R. YANG, M. GABBOUJ, AND Y. NEUVO, *Weighted median filters: a tutorial*, IEEE Trans. Circ. Syst. II, 43 (1996), pp. 157–192.
- [35] Y. YOU, W. XU, A. TANNENBAUM, AND M. KAVEH, *Behavioral analysis of anisotropic diffusion in image processing*, IEEE Trans. Image Process., 5 (1996), pp. 1539–1553.